

## **A SANS Study of Organoclay Dispersions<sup>1</sup>**

**H. J. M. Hanley,<sup>2,3</sup> C. D. Muzny,<sup>2</sup> D. L. Ho,<sup>4</sup> C. J. Glinka,<sup>4</sup>  
and E. Manias<sup>5</sup>**

---

Small-angle neutron scattering (SANS) is used to investigate the dispersion in toluene of various forms of the complex, Cloisite C15A. Cloisite is a commercially important exchanged clay prepared from montmorillonite and the cation di-tallow ammonium. Points discussed include estimates of the extent to which the complex is dispersed, the amount of organic clay platelet surface layer coverage, and possible network formation of the complex in the solvent. From power-law plots of the scattered neutron intensity versus the wave vector, it is estimated that C15A is well dispersed into clusters which consist of a stack of between three and seven di-tallow-coated montmorillonite platelets. The removal of excess di-tallow from the surface layer reduces the number of platelets in the cluster. Substitution of dimethyloctodecyl ammonium for the di-tallow molecule promotes network formation. It is demonstrated that SANS is a powerful tool for examining these complicated organic/inorganic systems.

---

**KEY WORDS:** clay nanomaterial; Cloisite C15A; clusters; dispersions; di-tallow; gel; montmorillonite; organic/inorganic complex; small-angle neutron scattering (SANS).

### **1. INTRODUCTION**

A typical polymer/clay nanocomposite is composed of a filler embedded in a polymerized medium [1]. The filler is an organoclay, usually a cationic

---

<sup>1</sup> Paper presented at the Fourteenth Symposium on Thermophysical Properties, June 25–30, 2000, Boulder, Colorado, U.S.A.

<sup>2</sup> Physical and Chemical Properties Division, National Institute of Standards and Technology, Boulder, Colorado 80305, U.S.A.

<sup>3</sup> To whom correspondence should be addressed. E-mail: howard.hanley@nist.gov

<sup>4</sup> NIST Center for Neutron Research, National Institute of Standards and Technology, Gaithersburg, Maryland 20899, U.S.A.

<sup>5</sup> Materials Science and Engineering Department, Pennsylvania State University, University Park, Pennsylvania 16802, U.S.A.

complex in which the clay's natural surface metal cations have been exchanged with an organic, cationic surfactant. The surfactant layer is organophilic allowing the inorganic clay to be dispersed in the organic polymer. It is well known that the mechanical and thermal characteristics of the nanocomposite itself depend largely on the degree to which this dispersion can take place. Optimum characteristics occur when the largest possible clay surface area is made available for cation exchange, when this surface area is maintained throughout the exchange process, and when it is maintained during the subsequent polymerization. Ideally, then, the clay mineral should be separated into its constituent platelets in the nanocomposite precursor state.

Small-angle neutron scattering (SANS) is an excellent tool to probe the degree of separation or dispersion of an exchanged clay mineral in a solvent, as several studies have demonstrated. SANS results to date, however, seem to be restricted to complexes in an aqueous medium [2], a surprising limitation considering that organically based systems are industrially more important and numerous. But, very recently, we reported [3] SANS intensity data from the commercial complex known as Cloisite C15A in toluene. Cloisite is the material prepared from montmorillonite and the cation di-tallow (a naturally occurring variant of dimethyloctodecyl ammonium).

In Ref. 3 we investigated 1 and 2% suspensions of Cloisite C15A. The results that are relevant here are as follows. First, the SANS measurements, reinforced by wide-angle *X*-ray scattering results, indicate that the complex is reasonably well dispersed in that it forms clusters made up of a stack of about three di-tallow-coated montmorillonite platelets. The height of these complexes is estimated to be about 19 nm. The SANS data are not very sensitive to estimates of the diameter of the major face of the platelets, but dynamic light scattering experiments suggest that their hydrodynamic diameter is about 260 nm. Atomic force microscopy (AFM) experiments [4] indicate that the platelets are larger, with approximate diameters of 0.4 to 1.0  $\mu\text{m}$ , but we consider these two size estimates to be within the relative uncertainties of both methods. Second, it was clear that small changes in the extent and nature of the clay platelet surface coverage played potentially a key role in the dispersion mechanism. This point is followed up in this paper. As in Ref. 3, our samples were 1 and 2% suspensions of C15A in toluene. Commercial Cloisite has an excess of surfactant di-tallow associated with a montmorillonite clay platelet. [An excess is defined as an amount exceeding the cation-exchange capacity (CEC) of the montmorillonite.] Here we investigated the dispersion and behavior of complexes prepared from di-tallow with any excess di-tallow removed (designated "pure di-tallow") and investigated the system when the di-tallow is

replaced by its pure synthetic counterpart, dimethyldioctodecyl ammonium (designated "2C18"). Our overall objective is to see if the information thus gained allows us to understand better the mechanism of aggregation and dispersion of complexes in organic solvents, and in organic molecules in general.

## 2. MEASUREMENTS

### 2.1. Materials

The clay materials used in this work were C15A, its variants, and the sodium montmorillonite base, designated CNa+. C15A and CNa+ are commercial products provided to us as powders by Southern Clay Products, Inc. [5]. The supplier synthesized C15A by exchanging the sodium ions of CNa+ with 125 meq/100 g of di-tallow. The di-tallow itself is a mixture of dimethyl ammonium surfactants with various carbon chain lengths: C<sub>18</sub> (65%), C<sub>16</sub> (30%), and C<sub>14</sub> (5%). Since the CEC of CNa+ is estimated to be 92 meq/100 g, the surface of C15A is covered, in principle, by about 130% of one CEC layer.

A nominal 1% by mass dispersion of CNa+ was prepared by adding the commercial powder to distilled water and stirring vigorously for 3 h. This dispersion was then sonicated for 20 min and lightly centrifuged for 5 min. The eluent was a clear and stable suspension. This suspension was then diluted to give two other dispersions of nominal clay content, 0.5 and 0.1%, by weight, respectively.

Suspensions of C15A in toluene, 1 and 2%, by mass, were prepared following the simple procedure recommended by the supplier. For example, for a 2% suspension, 1 g of C15A was added to 57.7 ml of toluene and the solution stirred for 30 min in a flask. At this point a small amount of methanol, equivalent to 30%, by mass, of the clay content (i.e., 0.379 ml), and 0.2 ml of water were added, and the mixture was stirred for an additional 30 min. The sample was then centrifuged and sonicated briefly. We observed that the suspension, although viscous, was clear and stable for several weeks, with no significant settling. The 1% suspension was made up by direct weighing in a similar manner.

Pure di-tallow was provided by Rheox [5], and dimethyldioctodecyl ammonium chloride was purchased from Aldrich [5]. The complexes with these surfactants were prepared by cation exchanging the commercial CNa+ with these pure surfactants and subsequently removing excess surfactant by refluxing with methanol for 3 days. The 1 and 2%, by weight, solutions of these materials in toluene were prepared by the procedure outlined for C15A. It turned out that the pure di-tallow suspensions were

viscous and tended to form a gel that could be broken only by sonification. The 2C18 systems were, however, gel-like throughout, and a fluid suspension was unobtainable.

To carry out SANS contrast matching experiments, the samples were also made up in deuterated (d-) toluene, and in mixtures of deuterated and protonated (h-) toluene, following the above procedure.

## 2.2. Neutron Scattering

Neutron scattering intensities from the CNa+ clay and the complex suspensions were obtained from the appropriate samples, loaded in 1-mm-gap thickness quartz cells, and placed in the beam of the 30-m NG7 SANS instrument at the National Institute of Standards and Technology Center for Neutron Research (NCNR). The spectrometer was configured with an incident neutron wavelength  $\lambda = 0.6$  nm and sample-detector distances of 1.2, 5.0, and 15.3 m, to give a wave-vector range  $0.02 < q \text{ (nm)}^{-1} < 1.2$ . Here  $q = |\mathbf{q}|$  and  $q = 4\pi \sin(\theta/2)/\lambda$ , with  $\lambda$  the incident neutron wavelength and  $\theta$  the scattering angle. Scattered neutrons were detected on the instrument's 2D position-sensitive detector. Because all measured scattering patterns were isotropic, the measured counts were azimuthally averaged. These averaged data were corrected for empty cell and solvent scattering and placed on an absolute scale by normalizing to the intensity obtained from a water standard [6].

## 2.3. Small-Angle Neutron Scattering Equations

The coherent contribution to the scattered intensity  $I(q)$  from a monodispersed suspension of  $N$  particles of volume  $V_p$  occupying volume  $V$  is proportional to the differential cross section per unit volume of the sample  $d\Sigma/d\Omega$  ( $\text{cm}^{-1}$ ) [7, 8]:

$$d\Sigma/d\Omega = (N/V) |F(\mathbf{q})|^2 S(\mathbf{q}) \quad (1)$$

This equation expresses the total coherent scattering in terms of a single-particle form factor,

$$F(\mathbf{q}) = \sum_j b_j \exp(i\mathbf{q} \cdot \mathbf{X}_j) \quad (2)$$

and the structure factor,  $S(\mathbf{q})$ , which accounts for interparticle interference. The term  $b_j$  in Eq. (2) is the neutron scattering length of nucleus  $j$ . One, however, often considers the scattering length density defined operationally

by  $\rho = \rho_{\text{mol}} \sum b_j N(j)$ , where  $\rho_{\text{mol}}$  is the molecular density and  $N(j)$  is the number of nuclei of type  $j$  in a particle.

Experimentally, scattering from a species is measured with respect to the scattering length density of the medium  $\rho_m$ . If this scattering length density difference is independent of the particle position, the cross section, and hence the scattered intensity, for a noninteracting system can be written in terms of the volume fraction  $\phi$ , where  $\phi = (N/V) V_p$ :

$$I(q) = A\phi V_p (\rho - \rho_m)^2 P(q) \quad (3)$$

where  $A$  is an apparatus constant.  $P(q)$  is the square of the orientationally averaged  $F(\mathbf{q})$  written in dimensionless form, a term that can be evaluated analytically if the geometry of the scatterers is known. Here we assume that the clay platelets can be approximated by disks, and for a disk of radius  $R$  and height  $2H$ , we have

$$P(q) = F(q)^2 = 4 \int_0^{\pi/2} f^2(q, \beta) \sin \beta d\beta \quad (4)$$

where

$$f^2(q, \beta) = \left( \frac{\sin^2(qH \cos \beta)}{(qH)^2 \cos^2 \beta} \right) \frac{J_1^2(qR \sin \beta)}{(qR)^2 \sin^2 \beta}$$

Here  $J_1$  is the first integer-order Bessel function and  $\beta$  is the angle between  $\mathbf{q}$  and the major axis of the disk. Equation (4) simplifies considerably if  $qH \ll 1$ . In this case the first term in the integral is equal to 1, so that the equation becomes:

$$P(q) = \frac{2}{(qR)^2} \left[ 1 - \frac{J_1(2qR)}{qR} \right] \quad (5)$$

For  $qR > 2$  the asymptotic formula

$$P(q) = \frac{2}{(qR)^2} \exp[-(qH)^2/3] \quad (6)$$

is a useful approximation. The equations imply that a plot of  $\log(I)$  versus  $\log(q)$  from a system of noninteracting disks will have a slope of  $-2$  over a range of  $qR$ .

In this work, the scatterers are clay platelets for which the surface sodium ions have been replaced by an organic interface, and the organoclay complex can be considered to be made up of a central core and a

surface coating. If this core has a characteristic scattering length density  $\rho_1$ , and the surface has a characteristic scattering length density  $\rho_2$ , the scattered intensity from a system of isolated particles is of the form [2]

$$I \sim \{(\rho_2 - \rho_m)[V_T F_T(q) - V_1 F_1(q)] + (\rho_1 - \rho_m) V_1 F_1(q)\}^2 \quad (7)$$

where  $V_1$  is the volume of the core and  $V_T$  is the total volume of the particle.

Equation (7) is too simplistic if the particles, although isolated as a whole, consist of stacked layers. Assuming that the nearest-neighbor distance between the platelets obeys a Gaussian distribution, Kratky and Porod [9] proposed an internal structure factor,  $S_s(q)$ :

$$S_s(q) = 1 + \frac{2}{N} \sum_{k=1}^N (N-k) \cos(kDq \cos \beta) \exp[-k(q \cos \beta)^2 \sigma_D^2 / 2] \quad (8)$$

Here  $N$  corresponds to the number of stacked platelets, and  $D$  and  $\sigma_D$  represent the nearest-neighbor center-to-center distance and its Gaussian standard deviation, respectively.

Having Eq. (8), the intensity for the stacked cluster is represented by

$$I \sim \int_0^{\pi/2} \{(\rho_2 - \rho_m)[V_T f_T(q) - V_1 f_1(q)] + (\rho_1 - \rho_m) V_1 f_1(q)\}^2 S_s(q) \sin \beta d\beta \quad (9)$$

Inspection of Eqs. (7) and (9) indicates that if the scattering length density of the medium is the same as that for the surface species 2, the SANS intensity pattern will be from the core. Similarly, if  $\rho_1 = \rho_m$ , the scattering power of the system is controlled by the surface.

Scattering lengths and scattering length densities, together with the molecular mass and the mass density of the components of the suspensions, are listed in Table I. The parameters for CNa+ are those for a clay mineral

**Table I.** Parameters for the CNa+ and the Complex Systems

	Molar mass (g)	Mass density (g · cm <sup>-3</sup> )	Scattering length (10 <sup>-12</sup> cm)	Scattering length density (10 <sup>10</sup> cm <sup>-2</sup> )
CNa+	359.4	2.66	8.647	3.86
Di-tallow+	545.6	0.9	-3.58	-0.35
Di-tallowCl	581.1	0.9	-2.62	-0.24
Di-C <sub>18</sub>	550.0	0.9	-3.71	-0.36
Toluene	92.0	0.867	1.665	0.90
d-Toluene	100.0	0.943	9.991	5.68
H <sub>2</sub> O	18.0	1.0	-0.168	-0.56

layer with the formula  $[\text{Si}_4\text{Mg}_{0.33}\text{Al}_{1.67}\text{H}_2\text{O}_{12}]\text{Na}_{0.33}^+$ . The parameters for the di-tallow assume the carbon chain breakdown discussed above, namely,  $\text{C}_{18}$  (65%),  $\text{C}_{16}$  (30%), and  $\text{C}_{14}$  (5%).

### 3. RESULTS AND DISCUSSION

#### 3.1. Montmorillonite, CNa+

We refer to Ref. 3 for a discussion of the SANS intensities measured from an 0.5% suspension of CNa+ in water. The power-law slope of the curve  $I(q)$  versus  $q$  was  $-2.2$ , a result consistent with the predictions of Eqs. (4) to (6), given that the sample is estimated by the manufacturer to be 20 to 30% polydisperse. The SANS data thus suggest that the unexchanged clay sample forms suspension of non interacting thin platelets. As noted in Section 1, while the SANS intensity curves do not appear to be sensitive to estimates of the diameter of the major face of the platelets, dynamic light scattering experiments suggest that their hydrodynamic diameter is about 260 nm. AFM experiments, however, indicate that the platelets are larger, with approximate diameters of 0.4 to 1.0  $\mu\text{m}$ . Wide-angle X-ray data indicate that 2H is approximately 1 nm.

#### 3.2. Commercial Cloisite C15A

Small-angle neutron scattering measurements were carried out on the 1 and 2% C15A samples in two solvents. The first set of SANS data was obtained with the Cloisite suspended in toluene. Scattering from the di-tallow is not completely contrasted out but is minor compared to that from the CNa+ core. The second set was obtained from a 50/50, by volume, d/h-toluene suspension. Here the scattering length density of the solvent is close to matching that of the core, so the scattered intensity is primarily that from the surfactant layer alone. The SANS intensity patterns for the 1 and 2% C15A systems are given in Ref. 3 and reproduced here in Figs. 1 and 2.

The scattering from the 2% suspensions displays power-law behavior over a wide range of the wave vector with a slope of  $-2.5$ , compared with  $-2.2$  associated with CNa+. For the 1% suspension the slope is slightly more negative, at  $-2.9$ .

The curves suggest a peak at  $q \sim 1.3 \text{ nm}^{-1}$ , absent in the corresponding plot for CNa+. A peak around this value of  $q$  may reflect the high- $q$  behavior of the form factor of a coated platelet [Eq. (7)], although such a

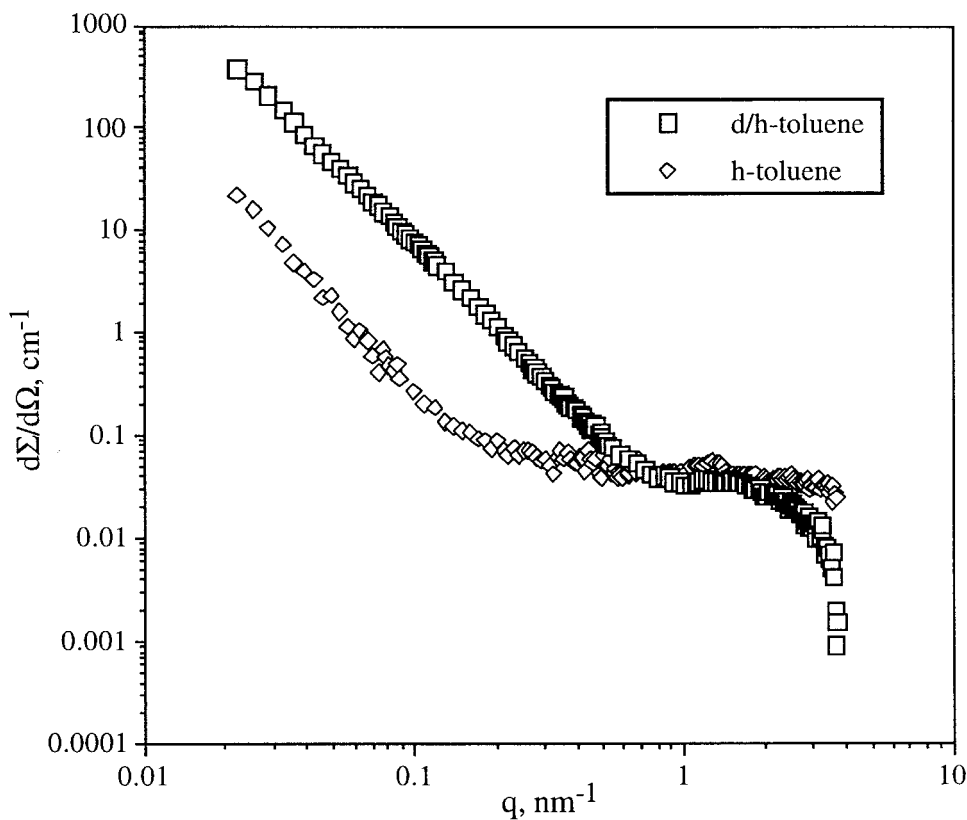


Fig. 1. SANS scattered cross sections from a 2% suspension of Cloisite C15A in h- and d/h-toluene.

peak would be softened by polydispersity. We note, however, that a peak is present in the SANS curves from the toluene suspensions and that these data were obtained from systems in which the surfactant was almost contrasted out. This being the case, the form factor is effectively that of an uncoated disk [Eq. (4)], that is, monotonically slowly decreasing in this  $q$ -range of interest. In our opinion, therefore, the peaks have a component that indicates a characteristic length in the system of about 5 nm, and this length represents the spacing between stacked surfactant-coated platelets. Wide-angle  $X$ -ray scattering experiments substantiated this point. As reported in Ref. 3, the complex C15A was investigated dry, as supplied by Southern Clay products, and as 1 and 2% suspensions of pure di-tallow in the toluene solvent. Evidence of three orders of primary spacing of about 4.5 nm was observed in the suspensions. Since the  $d$ -spacing between dry CNA+ was measured to be  $\sim 1.0$  nm, 4.5 nm corresponds to a single di-tallow layer thickness of about 1.75 nm. We would expect a similar thickness for the surface layers for our samples. Given the parameters listed in Table I, our curves for the 2% suspension were fitted to Eq. (9), using



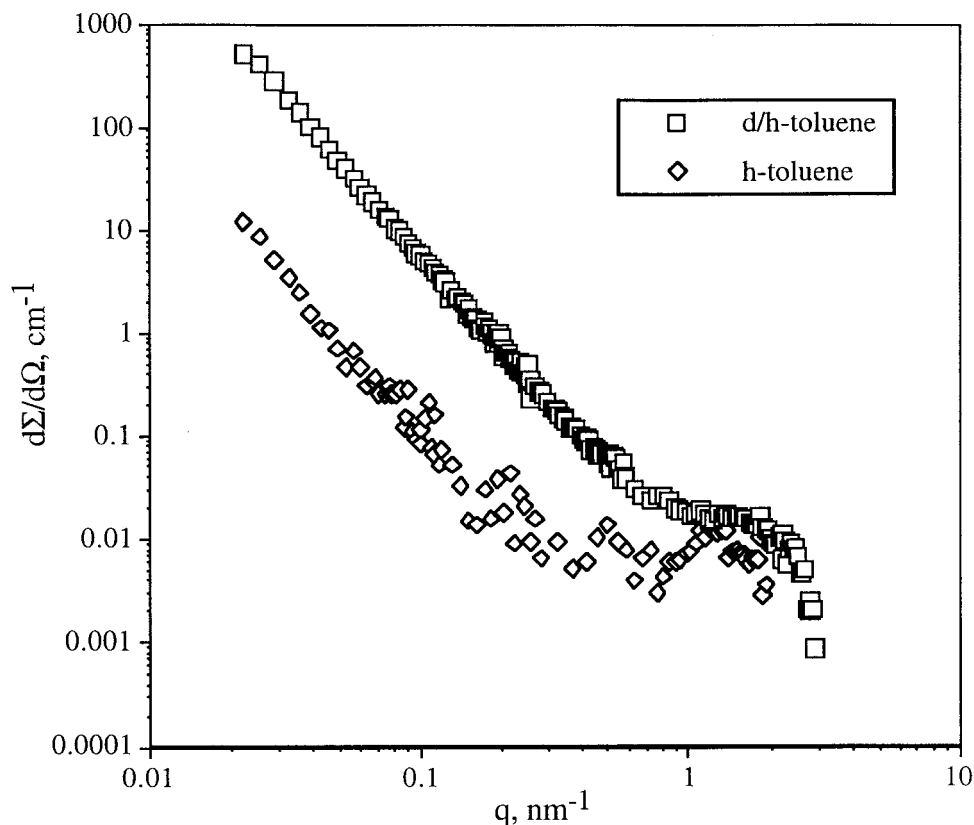


Fig. 2. SANS scattered cross sections from a 1% suspension of Cloisite C15A in h- and d/h-toluene.

Eq. (8). Details are given in Ref. 3. For toluene, best fits were obtained by fixing  $D = 5.0$  nm (corresponding to a layer thickness of 1.95 nm) and  $\sigma_D = 0.226$  nm; for d/h-toluene the values were  $D = 5.8$  nm (a layer thickness of 2.40 nm) and  $\sigma_D = 0.351$  nm. The fits yielded values for  $N$ , the number of plates in a cluster, of 3 and 7, respectively. The discrepancy between the two sets of data is somewhat wider than expected, but recall that the results are from the commercial samples with excess surfactant present: the amount of excess is dependent on the preparation history of the suspension and, quite possibly, on the small difference between h-toluene and d/h-toluene as the medium. See next section.

### 3.2.1. Surface Coverage

A method, introduced by Hanley et al. [2], that requires no assumptions of the surface morphology gives an estimate of surface coverage. A shift in the forward scattering for a sample in various solvents is proportional to the number of moles displaced by the scatterers. The scattering

power of, say, 1 mol of scatterer  $a$  that displaces  $x_{ab}$  mol of solvent  $b$ ,  $\Delta_{ab}$ , is

$$\Delta_{ab} = \left[ \sum_{ia} b_i - x_{ab} \sum_{ib} b_i \right]^2 \quad (10)$$

Supposing that 1 mol of scatterer  $a$  now has  $x_c$  mol of a surface compound  $c$  attached to it, and species  $c$  displaces  $x_{cb}$  mol of solvent  $b$ , the scattering power becomes

$$\Delta_{acb} = \left[ \left( \sum_{ia} b_i + x_c \sum_{ic} b_i \right) - \sum_{ib} b_i (x_{ab} + x_{cb}) \right]^2 \quad (11)$$

In our case, the unknown quantity is  $x_c$ , the number of moles of di-tallow that form the surface layer on 1 mol of CNa+. But this can be estimated from the ratio of the scattering power of C15A in the two solvents, toluene and d/h-toluene. If we assume that the surface layer is 1 CEC equiv of di-tallow+, Eq. (11) predicts a ratio between the scattered intensities from the sample in toluene and the 50% d/h-toluene mixture of approximately 25. If, however, we realize that the surface layer contains some di-tallow molecules (i.e., with Cl), the ratio calculated from Eq. (11) increases substantially. Specifically, if 0.1 mol of di-tallow is in excess (based on the supplier's estimate that the surface of dry C15A is covered to about 130% of one CEC layer), the ratio is about 250.

For the 1% suspensions (Fig. 2), the ratio at low  $q$  is  $\sim 60$ , a ratio that corresponds to an excess surface coverage of about 15%. We thus speculate that the toluene solvents are washing some of the excess di-tallow from the immediate clay surface of the complexes: a conclusion that is not unexpected. However, the experimental ratio for the 2% suspension is about 25 (Fig. 1). This value is very low. We have verified that the scattering from the dispersant in the toluene solvent is consistent with the amount of clay in suspension. Why there appears to be far less excess surfactant on the clusters of the 2% dispersion, with respect to the 1% dispersion, is not clear. But the 2% suspension is much more viscous. Hence the SANS calculation reinforces strongly the argument that the amount of excess surfactant plays a very significant role in the network or gel-like characteristics of the suspension on a longer length scale.

### 3.3. Pure Di-tallow

SANS data for pure 1 and 2% di-tallow dispersions in toluene and in the d/h-toluene mixture are displayed in Fig. 3. The slopes from the curves obtained in d/h-toluene are  $-2.5$  for both the 1 and the 2% dispersions.

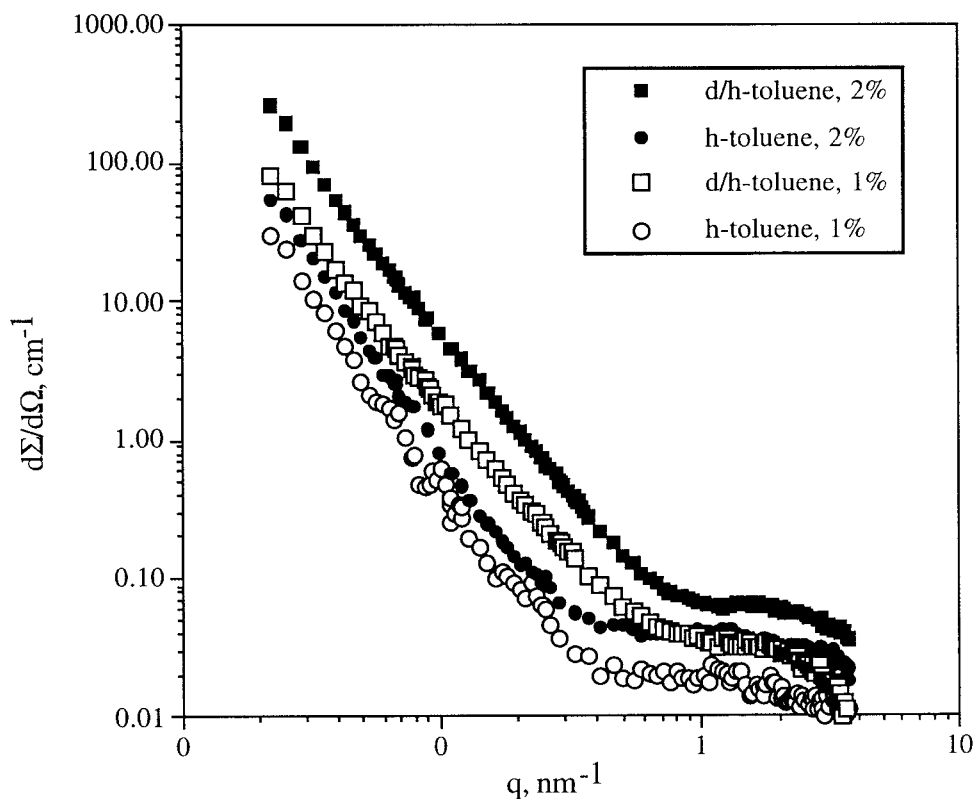


Fig. 3. SANS scattered cross sections from the complex prepared from pure di-tallow in h- and d/h-toluene.

Some structure at the higher  $q$  is evident, as shown in Figs. 1 and 2. The curves differ slightly from those in Figs. 1 and 2 in that the toluene results deviate slightly from a parallel pattern at a low  $q$ . Moreover, the displacement calculation method gives an unrealistically low surface-coverage estimate for these samples.

### 3.4. 2C18 Systems

Deviations from general power-law behavior are more apparent in the intensity patterns from the 2C18 suspensions (Fig. 4). It is very clear that, while the curves from the complex in the d/h-toluene suspension follow power-law behavior (with slopes of  $-2.5$ ), the curves for the complex in toluene display a rise at the lower  $q$ . We comment further on Fig. 4 in the next section.

## 4. CONCLUSION

In this paper we have considered three variants of organically modified montmorillonite (Cloisite) suspended in toluene: the commercial

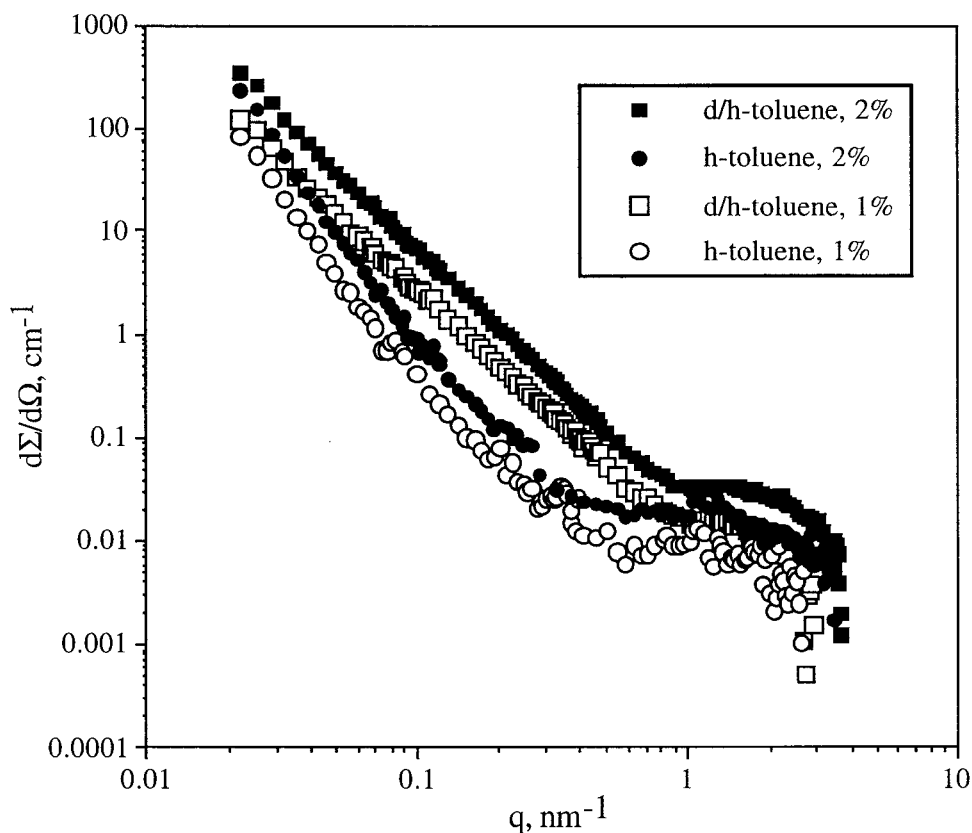


Fig. 4. SANS scattered cross sections from the complex prepared from 2C18 in h- and d/h-toluene.

product, which contains excess surfactant; the complex free of excess surfactant; and the complex prepared from dimethyloctodecyl ammonium chloride. The SANS data indicate that the clay platelets of these various Cloisites can be dispersed in toluene, only the platelets aggregate to form clusters.

An objective of this work was to see how modifying the surfactant surface layer of the exchanged clay might affect the dispersion. Our first conclusion stems from Fig. 5, which emphasizes the higher- $q$  behavior of the scattered intensities from the three samples in toluene. It is seen that the peak at  $q \sim 1.3$  decreases, and may move slightly to lower  $q$ , as the C15A sample is replaced by the excess-free sample, then by the 2C18. The Kratky and Porod internal structure factor [Eq. (8)] dominates since the form factor in toluene is well behaved and monotonically decreasing in this  $q$ -range. We conclude, therefore, that the number of platelets in the complex decreases as the system becomes more defined.

At this time, we cannot explain satisfactorily the contrast scattering behavior of the 2C18 complexes where the sets of curves (Fig. 4) display

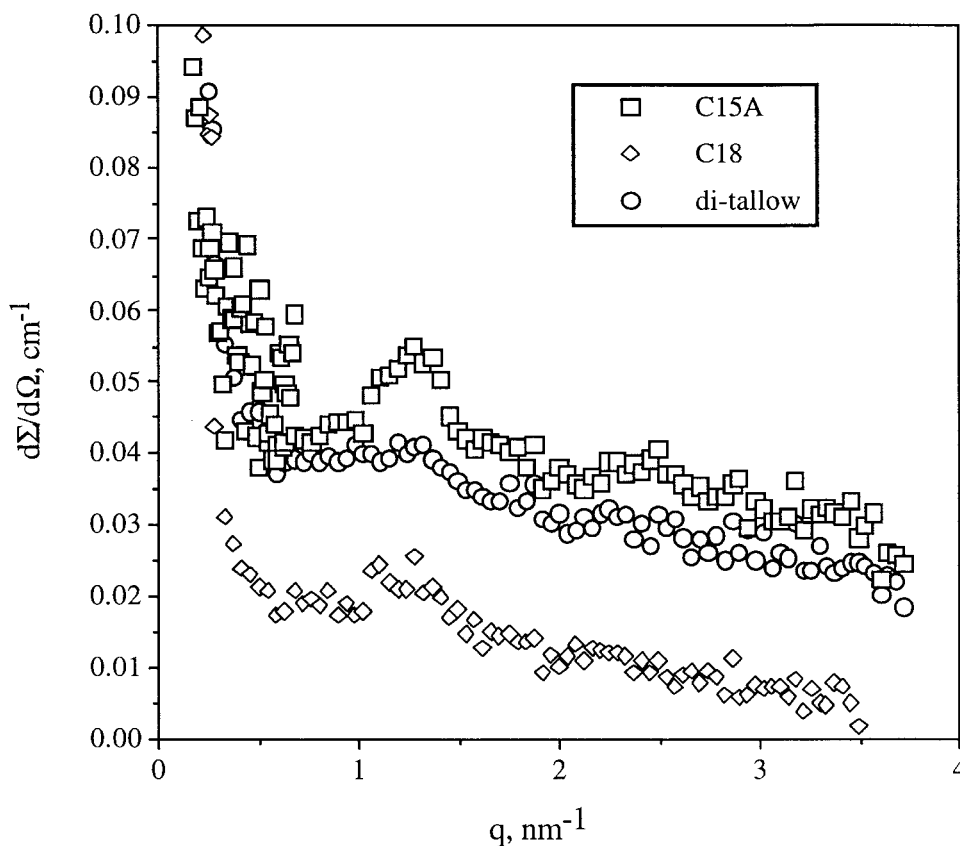


Fig. 5. The high- $q$  SANS scattered cross sections from the three Cloisites in 2% h-toluene.

different  $q$  dependences at low  $q$ . Further experiments with the 2C18 dispersions at other volume fractions verified that the experimental trends are correct. We can speculate only that the 2C18 surfactant is not coating all the clay platelets, hence, the scattering pattern has a contribution from this uncoated clay.

#### ACKNOWLEDGMENTS

The SANS data were taken on the NG7 30-m instrument at the NIST Center for Neutron Research. We thank the staff there for their encouragement and support. Part of this work was carried out at the Lucas Heights site of the Australian Nuclear Science and Technology Organization.

#### REFERENCES

1. E. P. Giannelis, R. Krishnamoorti, and E. Manias, *Adv. Polym. Sci.* **118**:108 (1999); M. Alexandre and P. Dubois, *Mater. Sci. Eng. Res.* **28**:1 (2000).

2. H. J. M. Hanley, C. D. Muzny, and B. D. Butler, *Langmuir* **13**:5276 (1997).
3. H. J. M. Hanley, C. D. Muzny, D. L. Ho, and C. J. Glinka (in preparation).
4. D. L. Ho, R. M. Briber, and C. J. Glinka, *Chem. Mater.* (in press).
5. Commercial names are used to identify the materials so that the experiments can be repeated if necessary. Their endorsement by the NIST is not implied.
6. C. J. Glinka, *J. Appl. Cryst.* **31**:430 (1998); Cold Neutron Research Facility at the NIST, NG3 and NG7 30-Meter SANS Instruments Data Acquisition Manual (1999).
7. S.-H. Chen and T.-S. Lin, *Methods in Experimental Physics, Vol. 23, Part B. Neutron Scattering*, D. L. Price and K. Skold, eds. (Academic Press, London, 1987).
8. J. S. Higgins and H. C. Benoit, *Polymers and Neutron Scattering* (Clarendon Press, Oxford, 1994).
9. O. Kratky and G. Porod, *J. Colloid Sci.* **4**:35 (1949).